Diazonium-Derived Aryl Films on Gold Nanoparticles: Evidence for a Carbon–Gold Covalent Bond

Lars Laurentius,[†] Stanislav R. Stoyanov,[‡] Sergey Gusarov,[‡] Andriy Kovalenko,[‡,§] Rongbing Du,[⊥] Gregory P. Lopinski,[⊥] and Mark T. McDermott[†,*]

[†]Department of Chemistry and National Institute for Nanotechnology, University of Alberta, Edmonton, Alberta, Canada, [‡]National Institute for Nanotechnology, Edmonton, Alberta, Canada, [§]Department of Mechanical Engineering, University of Alberta, Edmonton, Alberta, Canada, and [⊥]Steacie Institute for Molecular Sciences, Ottawa, Ontario, Canada

ABSTRACT Tailoring the surface chemistry of metallic nanoparticles is generally a key step for their use in a wide range of applications. There are few examples of organic films covalently bound to metal nanoparticles. We demonstrate here that aryl films are formed on gold nanoparticles from the spontaneous reduction of diazonium salts. The structure and the bonding of the film is probed with surface-enhanced Raman scattering (SERS). Extinction spectroscopy and SERS show that a nitrobenzene film forms on gold nanoparticles from the corresponding diazonium salt. Comparison of the SERS spectrum with spectra computed from density functional theory models reveals a band characteristic of a Au–C stretch. The observation of this stretch is direct evidence of a covalent bond. A similar band is observed in high-resolution electron energy loss spectra of nitrobenzene layers on planar gold. The bonding of these types of films through a covalent interaction on gold is consistent with their enhanced stability observed in other studies. These findings provide motivation for the use of diazonium-derived films on gold and other metals in applications where high stability and/or strong adsorbate–substrate coupling are required.

KEYWORDS: gold nanoparticles · diazonium salt · covalent modification · SERS · HREELS · DFT

Methods to functionalize nanoparticles are generally derived from schemes used for modifying macroscopic, planar substrates. The interaction between a substrate and adsorbate layer often controls the structure and properties of the layer and governs the types of applications for which the modified substrate can be employed. Covalent bonding between organic molecules and substrates such as silicon,[1] glass,[2] and carbon[3] is known. Electrochemical methods are used to chemically graft polymers to metal surfaces,[4] but in general, organic molecules covalently bound to metals are less prevalent. Organic molecular layers on noble metal surfaces have been used in a wide range of applications. The self-assembly of alkythiolate monolayers is the most broadly applied modification method for noble metals such as gold.[5,6] The monolayers are easily formed, are highly organized, and provide a pathway to create interfaces with a variety of functional groups. The interaction between the sulfur and gold is labile, which allows for the self-organization of this monolayer system but can also lead to instability under certain conditions.[6] Despite the noncovalent nature of the interaction, thiol-derived monolayers on gold are sufficiently stable to be widely applied in fundamental studies, biosensing, molecular electronics, and surface patterning.[5]

The modification of conducting surfaces with diazonium-salt-derived aryl layers has been gaining significant attention.[3,7] Diazonium salts are electrochemically or spontaneously reduced at the surface of a conductor to form an aryl radical that binds to the surface. These films tend to form multilayers and are relatively disordered.[8,9] The interaction between diazonium-derived aryl films and the substrate is very stable, able to withstand prolonged ultrasonic treatment, boiling in various solvents, and long time exposure to ambient conditions.[7] It is widely accepted that the interaction between diazonium-derived films and graphitic carbon substrates is a C–C covalent bond. This is supported by Raman spectroscopic evidence[10] and more recently by fragmentation patterns observed in time-of-flight secondary ion mass spectrometry experiments.[11] The bonding of diazonium-derived films on metal surfaces has been studied. Angle-resolved X-ray photoelectron spectroscopy (XPS) revealed the presence of a carbide layer at an aryl–Fe interface, suggesting a covalent bond on Fe.[12] Highly stable films have been reported on Cu surfaces, and XPS results indicated the presence of both Cu–O–C and Cu–C bonds.[13]

Several groups have reported on the formation of aryl films on gold surfaces *via* the reduction of diazonium salts.[14–19] The

* Address correspondence to mark.mcdermott@ualberta.ca.

Received for review March 24, 2011 and accepted April 26, 2011.

Published online April 26, 2011
10.1021/nn201110r

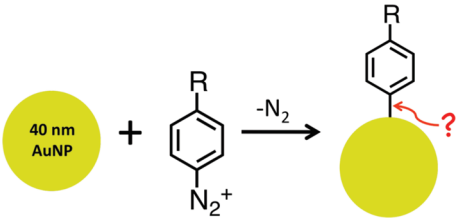

Scheme 1. Potential reaction between a gold nanoparticle and diazonium salt.

structure and stability of electrochemically deposited films are similar to those formed on carbon. We have shown that diazonium-derived nitrobenzene (dNB) films are more strongly bonded to gold surfaces than the thiol analogue.[19] Downard and co-workers have recently examined the formation of diazonium-derived layers on gold by spontaneous (open-circuit) adsorption.[20] It was shown that the growth of nitrobenzene films was dependent on incubation time and observed films ranging from a submonolayer to multilayers consisting of 2−3 layers.

The general understanding of the formation and structure of thiol-derived self-assembled monolayers on planar gold substrates opened pathways for the use of thiols in the modification of gold nanoparticles (AuNPs).[21,22] Following a similar train of thought, we envision the formation of aryl layers on AuNPs *via* the spontaneous reduction of diazonium salts. A general scheme of the potential reaction is shown in Scheme 1. Our efforts are focused on showing that this reaction takes place and in exploring the type of binding between the aryl groups and gold nanoparticles. The use of diazonium-derived films for the stabilization of metal nanoparticles has been examined by Schiffrin and co-workers, who reported on the synthesis of gold and platinum nanoparticles in the presence of diazonium salts.[23] They postulated that the formation of a gold−carbon bond would provide superior stability compared to metal−sulfur interactions. A similar process was used for the synthesis of aryl-stabilized palladium nanoparticles.[24] In both of these studies, the existence of a metal−C covalent bond was assumed but not proven. The use of diazonium salts for the modification of preformed nanoparticles has also been demonstrated. Mangeney *et al.* reported on the sonication-assisted, electroless modification of diamond nanoparticles with 4-nitrobenzene diazonium salt.[25]

We demonstrate here the functionalization of preformed, citrate-stabilized AuNPs by spontaneous adsorption of dNB, as shown in Scheme 1. We are motivated by the potential applications of nanoparticles with covalently bonded layers. In addition, this system will afford the ability to probe the aryl group−gold interactions by surface-enhanced Raman scattering (SERS). The combination of SERS and density functional theory (DFT) modeling is used to identify a Raman band associated with a Au−C stretch. This vibrational mode

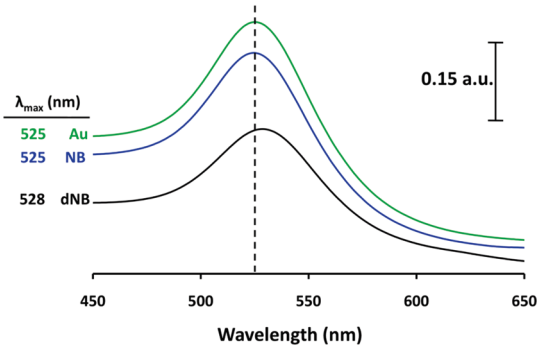

Figure 1. Extinction spectra of unmodified 40 nm AuNPs, AuNPs reacted with nitrobenzene (NB, control), and dNB-modified 40 nm AuNPs. All samples were suspended in water. The mean value for three measurements is shown. The uncertainty of the measurement (sd) is 0.3 nm.

is also observed on planar gold surfaces by high-resolution electron energy loss spectroscopy (HREELS). The observation of a Au−C vibrational band is the first direct evidence of a covalent bond in diazonium-derived aryl layers on noble metals.

RESULTS AND DISCUSSION

Previous reports have shown that aryl films can be formed on planar gold surfaces from the spontaneous adsorption of diazonium salts.[20,26] It has also been shown that metal nanoparticles can be stabilized during synthesis by a diazonium-derived layer.[23,24] It has not yet been demonstrated that diazonium salts will spontaneously adsorb to preformed gold nanoparticles (AuNPs). We describe here our results from spectroscopic studies that show aryl layers form on the surface of 40 nm AuNPs from the spontaneous adsorption of the corresponding diazonium salt. Vibrational spectroscopic data are used to probe the interaction between the aryl groups and AuNPs.

A strong absorption band, known as the localized surface plasmon resonance (LSPR), is observed in the visible spectrum of AuNPs. It is known that the position of this band is sensitive to the dielectric constant surrounding the nanoparticle and, thus, responds to surface modification. For example, the self-assembly of an alkanethiolate monolayer on silver nanoparticles was shown to red-shift the wavelength maximum (λ_{max}) of the LSPR.[27] The visible spectrum can also be used to monitor the stability and flocculation of nanoparticles in solutions.[27,28] Commercial 40 nm AuNPs were reacted with nitrobenzene diazonium cations (dNB) as well as nitrobenzene, for comparison. Figure 1 contains the extinction spectra centered around the LSPR bands for unmodified, citrate-capped 40 nm AuNPs and nanoparticles exposed to the various potential adsorbates. The λ_{max} values of the LSPR bands are also listed in Figure 1.

The band for the unmodified NPs exhibits a maximum at 525 nm. Nanoparticles reacted with NB yield a

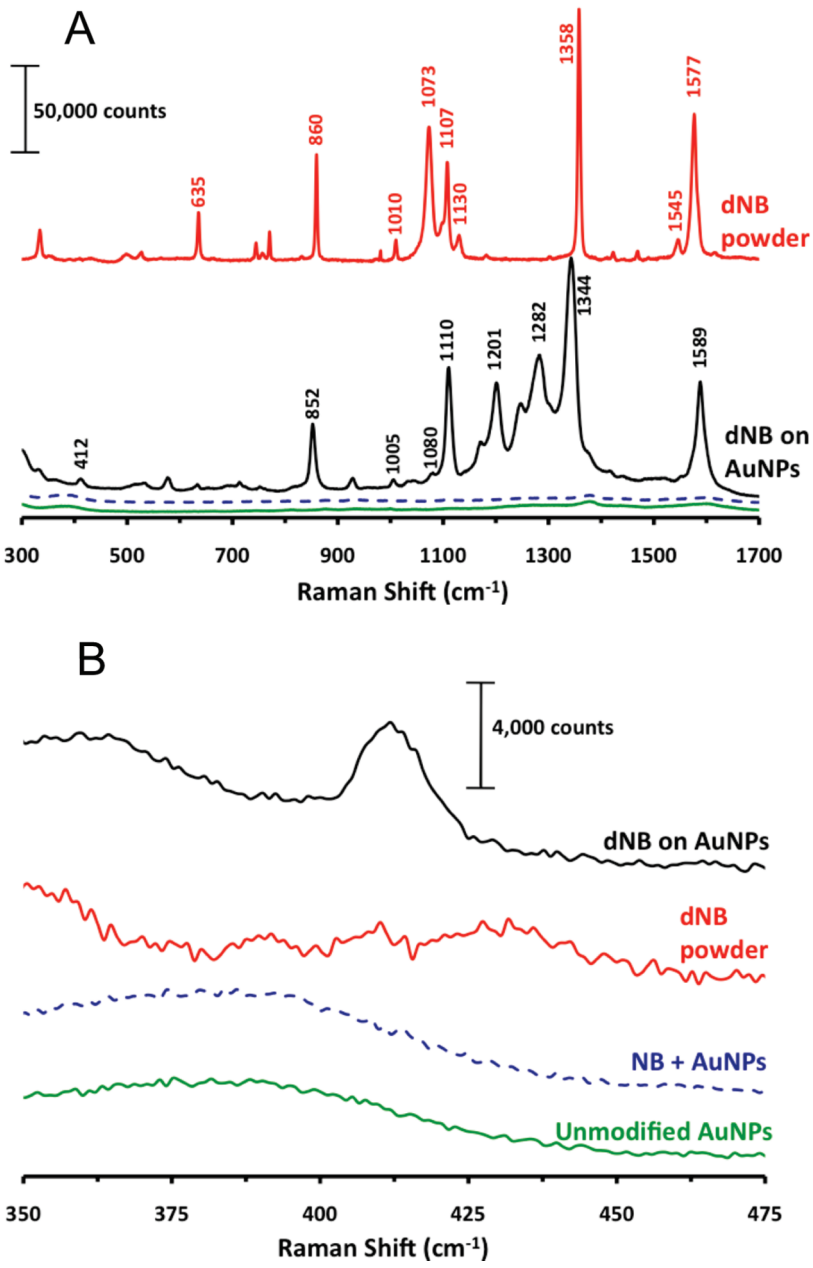

Figure 2. (A) Raman spectrum of solid dNB (top spectrum, red) and SERS spectra of dNB-modified 40 nm AuNPs (solid black line), 40 nm AuNPs reacted with NB (dashed blue line), and unmodified 40 nm AuNPs (solid green line). (B) Raman and SERS spectra of all the samples in (A) expanded near 400 cm^{-1}.

λ_{max} that is indistinguishable from unmodified AuNPs, implying there is negligible physisorption through the aromatic ring or the nitro group. The band position for NPs reacted with dNB is located at 528 nm, red-shifted significantly from that for unmodified NPs. This shift in λ_{max} is consistent with the formation of an adsorbate layer on the surface of the nanoparticles. We note that the intensity of the LSPR band for the dNB-modified AuNPs is lower than that for the unmodified AuNPs. This is due to loss of a portion of the AuNPs during separation of the modified nanoparticles from unreacted diazonium salt *via* centrifugation. However, the dNB-modified AuNPs that are resuspended remain stable in the aqueous solution. The spectrum in Figure 1 provides no indicators of nanoparticle aggregation as we observe no absorption bands in the region between 600 and 800 nm. We have found that 40 nm AuNPs modified with dNB are stable in solution for at least 1 month with no evidence of aggregation. We conclude from Figure 1 that reaction of dNB with AuNPs results in the formation of an adsorbed layer on the nanoparticle surface.

We have further characterized the diazonium-derived layers on AuNPs with SERS. Gold nanoparticles with diameters in the 20−100 nm range are excellent substrates for SERS.[29] In addition, NB and NB-containing

TABLE 1. Band Assignments Listed for the Raman Spectrum of Solid dNB and the SERS Spectrum of NB on the Surface of 40 nm AuNPs (References 30 and 31 Were Used for Some Assignments)

	band position (cm^{-1})	
assignment	dNB powder	dNB on AuNPs
N≡N stretch	2309	
ring stretch	1577	1589
asymmetric NO_2 stretch	1545	
symmetric NO_2 stretch	1358	1344
C—N_2 stretch	1130	
C—N stretch + ring stretch	1107	1110
CH i.p. bend	1073	1080(w)
ring breathing	1010	1005(w)
ONO scissor + ring stretch	860	852
asymmetric Ar C—C stretch + C—N—N i.p. deformation	635	

films have been the subject of a number of normal Raman[30] and SERS investigations.[22,31] In addition to providing structural information of an adsorbed layer, vibrational spectroscopy is particularly useful for probing the nature of the bonding between various adsorbates and gold substrates; a number of studies have reported evidence of a carbon—gold covalent bond. Recently, infrared photodepletion spectroscopy was used to study gold cluster carbonyls. The vibrational spectra obtained show Au—CO stretching and Au—C—O bending bands between 250 and 400 cm^{-1}.[32] Cyanide adsorption to gold has been probed with SERS. One study observed a band at 375 cm^{-1}, which was tentatively assigned to $Au(CN)_2^-$.[33] Other investigations have reported a Au—C stretching mode for Au—CN at 370 cm^{-1}.[34—36]

Figure 2A contains the Raman spectra in the region between 300 and 1700 cm^{-1} for the various NB—AuNP combinations as well as the normal Raman spectrum of dNB powder. The spectra for the two control samples (unmodified and NB) exhibit no major bands, consistent with negligible physical adsorption of NB to Au nanoparticles. The spectrum of the dNB-modified AuNPs is significantly enhanced and features numerous bands that are consistent with those observed in the dNB powder spectrum. Band assignments are listed in Table 1. The relative intensities of some of the more prominent bands as well as band positions in the SERS spectrum agree well with the dNB powder spectrum. Despite these similarities, there are notable differences between the two spectra. First, bands in the powder spectrum associated with the diazonium moiety are not observed in the SERS spectrum. A strong band is observed in the powder spectrum at 2309 cm^{-1} (not shown), which corresponds to the N≡N stretch of the diazonium group. This band is not observed in the SERS spectrum of dNB on AuNPs. In addition, bands at 1130 and 635 cm^{-1} in the dNB powder spectrum also involve the diazonium moiety (Table 1) and are not observed in the SERS spectrum. Taken together, these observations are strong evidence for spontaneous reduction of the diazonium cation to the aryl radical and the formation of a NB layer at the AuNP surface.

A second major difference in the spectra in Figure 2A is evident in the region between 1200 and 1300 cm^{-1}. The SERS spectrum of dNB on AuNPs exhibits bands at 1201, 1250, and 1282 cm^{-1} that are not present in the dNB powder spectrum. We believe these bands are due to the multilayer nature of the dNB film on the AuNPs, and assignment of these bands will be discussed below. Finally, a low intensity band at 412 cm^{-1} is observed in the dNB spectrum. This band is highlighted in the expanded region of the spectra in Figure 2B. A band centered at 412 cm^{-1} is clearly present in the dNB spectrum and not in the spectra of the powder or either of the control spectra. We have also observed this band in SERS spectra of other diazonium salts spontaneously adsorbed to AuNPs. A band for nitroazobenzene diazonium salt on 40 nm AuNPs appears at 416 cm^{-1}, and a band at 410 cm^{-1} is observed for phenyl acetic acid diazonium salt. As noted above, previous work has assigned bands at 375 cm^{-1} to a Au—C stretch for Au—CN. We thus tentatively assign the band at 412 cm^{-1} observed in Figure 2B to a Au—C stretch. The modeling studies described below support this assignment.

It is well accepted that electrochemically deposited diazonium-derived layers are bound to carbon materials through a C—C covalent bond.[7] Although it has been shown that these types of aryl films are strongly bonded to gold and other metals[13,19] and a Au—C bond has been predicted computationally,[37,38] direct spectroscopic evidence of a Au—C covalent bond has not yet been reported. The attachment and configuration of phenyl groups to gold have been previously explored using density functional theory (DFT). It has been predicted using DFT that the bond between the phenyl group and the gold surface is chemical in nature and that the upright configuration of the phenyl ring is favored.[37] Other modeling efforts have used and optimized DFT calculations to compliment SERS experimental results.[39] Schatz and co-workers have developed a time-dependent DFT method for calculating SERS enhancement factors and predicting band positions. The model is based on a pyridine molecule adsorbed to a 20 atom silver cluster.[40,41] Building upon these previous reports, we model dNB adsorbed to gold nanoparticles as a NB molecule covalently bonded to the vertex of a Au_{20} pyramidal cluster and label it Au_{20}vNB (Figure 3). The effect of NB multilayer formation on Raman spectra is modeled by a NB trimer bonded to the vertex of a Au_{20} cluster, labeled as Au_{20}vNB_3. In Figure 3, we show the optimized geometries of the structures containing NB and NB_3 bonded to the vertices of Au_{20} pyramids. Binding configurations

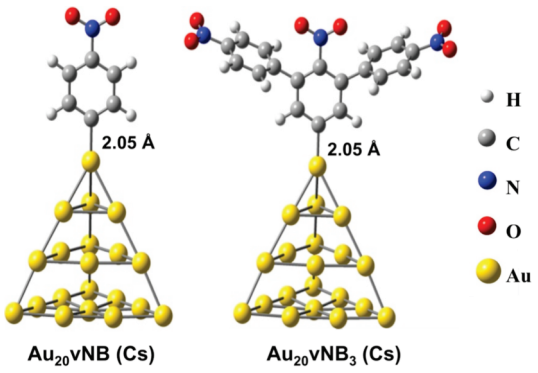

Figure 3. Optimized structure of a nitrobenzene monomer (Au_{20}vNB) and trimer (Au_{20}vNB$_3$) covalently bonded to pyramidal Au_{20} clusters.

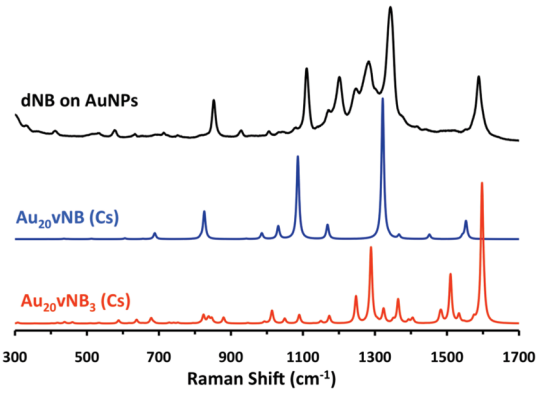

Figure 4. Calculated Raman spectra (Gaussian 09) of Au_{20}vNB and Au_{20}vNB$_3$ compared to the SERS spectrum of dNB bonded to AuNPs.

containing NB and NB$_3$ covalently bonded to the vertex of the Au_{20} pyramid are more stable by 44 and 39 kJ/mol, respectively, than the configurations bonded to the face of the pyramid. Optimization of structures containing NB bonded to the rim of the Au_{20} pyramid converges to either a vertex or a surface-bonded structure. The optimized Au−C bond lengths are 2.05 Å for both Au_{20}vNB and Au_{20}vNB$_3$.

The calculated Raman spectra for the model systems as well as the experimental SERS spectrum of dNB on AuNPs are shown in Figure 4. The electronic absorption maximum for nitrobenzene is 263 nm, and we do not expect any resonance Raman effects with the 785 nm excitation used here. Thus, the Raman scattering intensities for the model systems were calculated for the static case (ω = 0). Band assignments for the two models as well as the experimental SERS spectrum are listed in Table 2. Qualitatively, in terms of relative band intensities and band positions, the spectrum derived from the Au_{20}vNB model agrees more closely to the experimental SERS spectrum. This implies that the majority of the nitrobenzene molecules bound to the 40 nm AuNPs are in a single layer. The spectrum yielded by the Au_{20}vNB$_3$ model contains a number of additional modes assignable to the NB groups in the

TABLE 2. Assignment of Raman Bands from the SERS Spectrum and from Calculated (Gaussian 09) Spectra of the Au_{20}vNB and Au_{20}vNB$_3$ Structures

	band position (cm^{-1})		
assignment	SERS dNB on AuNPs	Au_{20}vNB	Au_{20}vNB$_3$
ring stretch	1589	1553	1598, 1510
symmetric NO_2 stretch	1344	1322	1365, 1325
ring breathing	1282, 1250	1277 (weak)	1289, 1248
C−H i.p. bend	1201, 1170	1169	1174, 1152
C−N stretch + ring stretch	1110	1086	1091
ONO scissor + ring stretch	852	836	825
Au−NB stretch	412	439	414

second layer. Of particular interest are ring breathing modes for the second layer of NB groups at 1289 and 1248 cm^{-1}. These modes agree well with bands observed at 1282 and 1250 cm^{-1} in the SERS spectrum. Multiple bands for in-plane C−H bending modes in the spectrum of Au_{20}vNB$_3$ are also consistent with the SERS spectrum. A number of other bands predicted for Au_{20}vNB$_3$ are not observed in the SERS spectrum. These differences may be due to the structure of the branched units in the dNB layer on the AuNPs relative to the model trimer structure. The model also does not account for coverage effects, which will certainly influence the bands observed in the SERS spectrum. Despite this, the agreement of the SERS spectrum with the calculated spectra of the two model structures is consistent with a diazonium-derived NB film bound to the AuNPs that contains branched multilayer structures.

A number of reports have addressed the interaction between diazonium-derived films and metals based on the stability of the film to various treatments.[13,15,18,19] We and others have previously shown that electrochemically deposited dNB remains bound to planar gold surfaces following severe ultrasonic treatment[15,19] and exposure to boiling solvents.[19] In addition, the dNB layer cannot be entirely displaced by long chain alkane thiols that completely displace a mercaptonitrobenzene monolayer. Recently, it was shown that a portion of a spontaneously adsorbed dNB film on planar gold remains following ultrasonic treatment in acetonitrile.[20] It has been suggested that these observations were due to a covalent linkage between the diazonium-derived film and the gold surface. However, direct evidence of a Au−C covalent bond has not yet been reported. The calculated Raman spectra from the two model systems both contain bands due to modes involving a Au−C stretch. As listed in Table 2, this band appears at 439 cm^{-1} for Au_{20}vNB and 414 cm^{-1} for Au_{20}vNB$_3$. The modes responsible for these bands are shown in Figure 5. As noted above, we observe a band at 412 cm^{-1} in the SERS spectrum of dNB on AuNPs that is observed in neither the Raman spectrum of the dNB starting material nor the control spectra. There are also no other bands in that vicinity of the SERS spectrum.

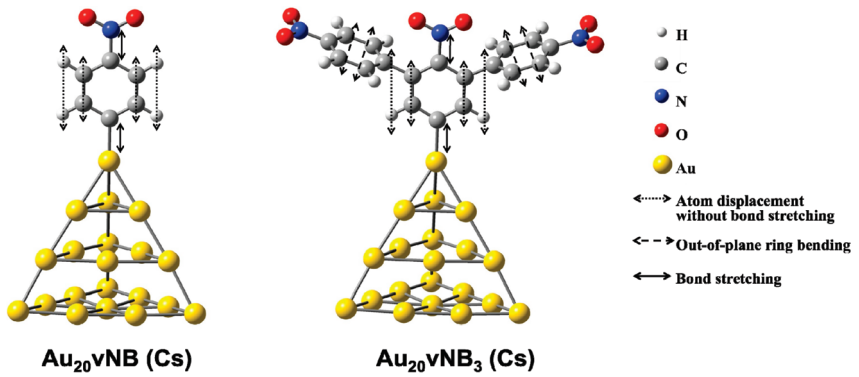

Figure 5. Illustration of the calculated (Gaussian 09) vibrational modes at 439 cm^{-1} ($Au_{20}vNB$) and 414 cm^{-1} ($Au_{20}vNB_3$) that involve Au−C bond stretching coupled with out-of-plane aromatic ring bending modes.

We thus assign the 412 cm^{-1} band to a mode involving a Au−C stretch as predicted in the Raman spectra of our models. This provides direct evidence for the existence of a Au−C covalent bond for this system.

The observation of a Au−C stretch in SERS spectra is compelling evidence for the existence of a gold−carbon covalent bond in diazonium-derived films on nanoparticles. Confirmation that this mode of bonding occurs on planar surfaces requires a highly surface-sensitive vibrational spectroscopic method. We thus studied dNB films on single-crystal Au(111) surfaces with high-resolution electron energy loss spectroscopy (HREELS). In HREELS, vibrational modes of adsorbed molecules can be identified by analyzing the energy loss of inelastically scattered electrons. Dipole-active modes tend to dominate HREELS spectra in the specular scattering geometry; however, non-dipole-active modes can be observed, as well. Thus, HREELS spectra are very comparable and complementary to SERS spectra.

Figure 6 contains HREELS spectra for Au(111) modified with dNB by both electrochemical grafting and spontaneous adsorption. The bottom spectrum in Figure 6 is that for the electrochemically deposited film plotted at full-scale and showing the relative intensities between the elastically scattered and inelastically scattered electrons. The signal intensities for the other two spectra in Figure 6 were normalized to the elastic bands and were expanded for clarity. The electrochemically deposited film yields bands at 1524, 1342, 1102, 845, and 420 cm^{-1} in the region shown. The band at 845 cm^{-1} is assigned to the ring stretch + ONO scissor mode and is in good agreement with the SERS peak observed at 852 cm^{-1}. The 1102 cm^{-1} band is assigned to a mode involving a ring stretch and a C−N stretch (Table 1). The bands at 1342 and 1524 cm^{-1} are assigned to symmetric and asymmetric NO_2 stretching based on previous publications.[19,42] The peak observed at 420 cm^{-1} is assigned to the Au−C stretch due to its proximity to the 412 cm^{-1} band in the SERS spectra.

The bands due to inelastic scattering for the spontaneously adsorbed dNB are much less intense than

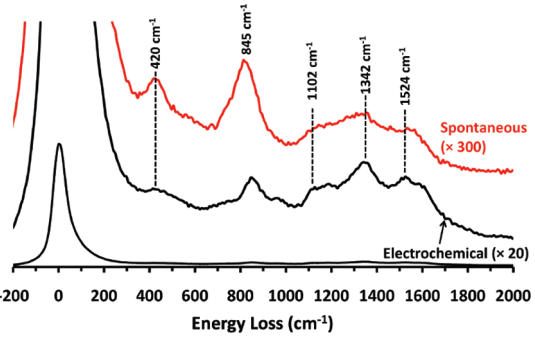

Figure 6. HREELS spectra for dNB films on Au(111) by spontaneous adsorption (top, red curve) and electrochemical grafting (middle and bottom, black curve). The lower spectrum is for the electrochemically deposited film plotted at full scale. The other spectra are plotted with expanded *y*-axis to better observe the vibration bands.

those for the electrochemically deposited film. On the basis of our previous work, we expect that the conditions used here for electrochemical deposition results in a dense, multilayer film of dNB with a thickness of ~2 nm. Since, in general, the inelastic scattering intensity will increase with surface coverage, the lower loss peak intensities observed for the spontaneous adsorbed film indicate that the coverage of dNB groups is substantially lower than the electrochemically deposited film. Despite the difference in coverage, the HREELS spectrum for the spontaneously adsorbed dNB film contains bands with similar position as the electrochemically deposited film. An interesting observation is the higher relative intensity of the band at 420 cm^{-1} in the spectrum of the spontaneously adsorbed film. We believe the enhanced intensity of this mode results from a relatively thin spontaneously adsorbed film compared to the electrochemically deposited film. A less intense band for a mode located at the metal−film interface is expected for a thicker, multilayer film due to the limited probing depth of the electrons. This observation also provides support for our assignment of the 420 cm^{-1} band to a Au−C stretching vibration. We thus conclude that a Au−C covalent bond is formed upon either spontaneous

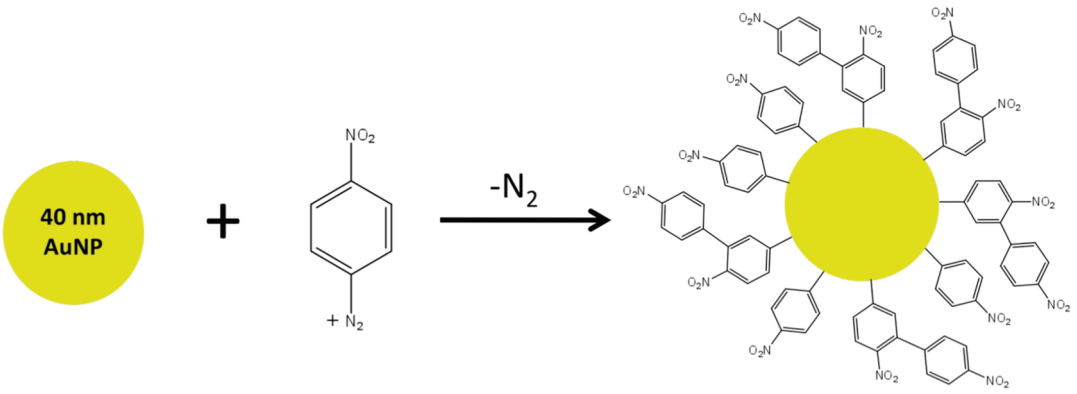

Scheme 2. Reaction scheme for the spontaneous adsorption of dNB to 40 nm AuNPs illustrating the proposed film structure on the surface of the nanoparticle.

adsorption or electrochemical grafting of dNB to Au(111).

CONCLUSIONS

The results presented here show that aryl films can be formed on gold nanoparticles by the spontaneous adsorption of diazonium precursors. Nanoparticles modified with diazonium-derived nitrobenzene yield excellent quality SERS spectra. Both UV–visible extinction spectroscopy and SERS are consistent with the formation of a nitrobenzene layer. The nitrobenzene-modified nanoparticles are stable in solution for at least 1 month. Comparison of the SERS spectrum with Raman spectra from DFT modeling indicates a degree of multilayer formation on the nanoparticles. The results are consistent with a reaction such as that shown in Scheme 2. Although Scheme 2 implies propagation of the multilayer solely through aryl–aryl attachment, propagation *via* radical attack of the nitro group is also a possibility. Importantly, the DFT modeling leads to the assignment of a SERS observed band at 412 cm^{-1} to a Au–C stretching mode. This is the first direct evidence of a gold–carbon covalent bond in these systems. Results from HREELS experiments confirm the existence of a Au–C bond for diazonium-derived films on planar surfaces. The anchoring of these types of films through a covalent interaction explains their enhanced stability compared to thiol-derived monolayer analogues. Diazonium-derived films on gold and other metals will continue to find applications where high stability and/or strong adsorbate–substrate coupling are required.

METHODS

Reagents and Materials. 4-Nitrobenzenediazonium tetrafluoroborate (dNB, 97%), silver nitrate (99%), and tetrabutylammonium tetrafluoroborate ($TBATF_4$) were obtained from Sigma-Aldrich and used as received. Nitrobenzene (NB, 99%) was purchased from Fisher Scientific. Reagent grade acetonitrile (CH_3CN) was purchased from either Caledon Laboratories or ACP Chemicals Inc. Anhydrous ethyl alcohol was obtained from Commercial Alcohols. Sulfuric acid (96%) and hydrogen peroxide (30%) were obtained from Mallinckrodt. The 40 nm citrate-capped gold nanoparticles (AuNPs) were purchased from BBInternational with a concentration of 9×10^{10} particles/mL. Deionized water with a resistivity of 18 MΩ or better was filtered in a Barnstead Nanopure purification system.

Gold Nanoparticle Modification. The 40 nm AuNPs were modified by mixing 10 μL of 2 mM 4-nitrobenzenediazonium tetrafluoroborate in acetonitrile with 1 mL of citrate-capped gold nanoparticle solution. Control samples were prepared by adding 10 μL of 2 mM nitrobenzene in acetonitrile to 1 mL of AuNPs. The reagents were left to incubate for 24 h after which time the nanoparticles were separated from solution *via* centrifugation at 8000 rpm for 10 min in an Eppendorf a5417R microcentrifuge. Next, the AuNP pellet was redispersed in 1 mL of deionized water. A second centrifugation step was added to wash the particles further. The suspended modified particles are stable and stored at 7 °C until use.

Extinction Spectroscopy. All nanoparticle solutions were diluted by a factor of 4 with deionized water before analysis. The extinction spectra were obtained in transmission mode on a double-beam Perkin-Elmer Lambda 35 instrument.

Raman Spectroscopy. The gold nanoparticles were analyzed by surface-enhanced Raman scattering (SERS). A 20 μL volume of the modified AuNPs was deposited on a gold-coated 3 × 1 in. premium microscope slide (Fisher Scientific) and analyzed. SERS spectra were recorded with a Renishaw inVia Raman microscope. Radiation of 785 nm from a high-performance, air-cooled diode laser was used for excitation. The integration time for the Raman spectrum of solid dNB was 10 s with a 17 ± 0.5 mW laser power at the sample. The SERS spectra of dNB-modified 40 nm AuNPs, 40 nm AuNPs reacted with NB, and unmodified 40 nm AuNPs were integrated for 30 s, and the laser power at the sample was 5 ± 0.5 mW. A Molectron Power Max 5100m was used to measure the laser power at the sample. All spectra were collected with a 50× objective. Care was taken to deposit equivalent amounts of particles on the slide and to focus the laser beam in areas of similar nanoparticle density for each sample.

High-Resolution Electron Energy Loss Spectroscopy (HREELS). A polished Au (111) single-crystal disk oriented to within 0.5° of the (111) plane (metal crystals and oxides) was cleaned in 3:1 v/v concentrated H_2SO_4/30% H_2O_2 at 120 °C for 30 min, followed by copious rinsing with Milli-Q water. *(The concentrated H_2SO_4: H_2O_2 piranha solution is very dangerous, particularly in contact with organic materials, and should be handled with extreme care).* Then the electrode was continuously cycled in aqueous 0.5 M H_2SO_4 solution between 0 and 1.75 V (SHE) at 100 mV/s until repeatable cyclic voltammograms were obtained. Cycling was halted and then maintained at 0 V for 60 s in order to obtain an

oxide-free surface. Electrochemical grafting employed an Autolab PGSTAT potentiostat (Eco Chemie, Utrecht, The Netherlands), a homemade reference electrode consisting of a silver wire submerged in a 0.01 M $AgNO_3$ solution in acetonitrile with 0.1 M tetrabutylammonium tetrafluoroborate ($TBABF_4$), and a platinum wire as the counter electrode. Electrochemical grafting was carried out using three full sweeps from 400 to −600 mV at a sweep rate of 200 mV/s and a diazonium salt (4-nitrobenzenediazonium tetrafluoroborate) concentration of 2.5 mM in acetonitrile with 0.1 M $TBABF_4$. Diazonium salt solutions were deaerated for 10 min with Ar gas prior to depositions. Spontaneous grafting was carried out by immersing cleaned Au substrates in a 1 mM solution of the diazonium salt in acetonitrile in the dark for at least 24 h. After the molecular grafting, the modified Au samples were rinsed and sonicated for 30 min in acetonitrile to remove the residual diazonium salt and the physisorbed materials.

The modified Au sample was attached to a molybdenum plate sample holder with a tungsten filament behind the sample to enable radiative heating. Upon transfer to the ultrahigh vacuum system (UHV), samples were heated to less than 400 °C to remove physisorbed species. HREELS was carried out with an LK Technologies LK3000 spectrometer. Spectra were acquired in the specular geometry (60° with respect to the surface normal) at an incident beam energy of 6 eV and a nominal spectrometer resolution of 6 meV (56 cm^{-1}).

Computational Techniques. The geometry optimization of $Au_{20}NB$ and $Au_{20}NB_3$ in C_S symmetry was performed using the Becke−Perdew (BP86) exchange-correlation functional,[43,44] as implemented in the Gaussian 09 computational chemistry package.[45] The BP86 functional often yields harmonic frequencies that are close to the experimental values.[41,46] For comparison, the PBE1PBE functional is also employed.[47] The $Au_{20}NB$ and $Au_{20}NB_3$ contain an odd number of electrons, and the electronic structures are modeled as unrestricted using double determinants. The Stuttgart−Dresden (SDD) effective core potential (ECP) was used for relativistic treatment of the [$1s^2$-$4f^{14}$] core electrons of Au.[48] The (8s7p6d)/[6s5p3d] Gaussian-type orbital (GTO) was applied for the valence shell of Au. The all-electron double-ζ basis set 6-31G* is used for O, N, C, and H atoms.[49,50] The Raman polarizability derivatives were calculated by numerically differentiating the analytic dipole derivatives with respect to an electric field.

Acknowledgment. This work was supported by the National Research Council (NRC) of Canada through the National Institute for Nanotechnology (NINT) and the Steacie Institute for Molecular Sciences (SIMS). We also acknowledge the Natural Sciences and Engineering Research Council of Canada (NSERC) for support. We thank the Western Canada Research Grid (WestGrid) and the NINT High-Performance Computing Facility for computational resources.

REFERENCES AND NOTES

1. Buriak, J. M. Organometallic Chemistry on Silicon and Germanium Surfaces. *Chem. Rev.* **2002**, *102*, 1271–1308.
2. Ulman, A. Formation and Structure of Self-Assembled Monolayers. *Chem. Rev.* **1996**, *96*, 1533–1554.
3. Downard, A. J. Electrochemically Assisted Covalent Modification of Carbon Electrodes. *Electroanalysis* **2000**, *12*, 1085–1096.
4. Palacin, S.; Bureau, C.; Charlier, J.; Deniau, G.; Mouanda, B.; Viel, P. Molecule-to-Metal Bonds: Electrografting Polymers on Conducting Surfaces. *ChemPhysChem* **2004**, *5*, 1468–1481.
5. Love, J. C.; Estroff, L. A.; Kriebel, J. K.; Nuzzo, R. G.; Whitesides, G. M. Self-Assembled Monolayers of Thiolates on Metals as a Form of Nanotechnology. *Chem. Rev.* **2005**, *105*, 1103–1169.
6. Vericat, C.; Vela, M. E.; Benitez, G.; Carro, P.; Salvarezza, R. C. Self-Assembled Monolayers of Thiols and Dithiols on Gold: New Challenges for a Well-Known System. *Chem. Soc. Rev.* **2010**, *39*, 1805–1834.
7. Pinson, J.; Podvorica, F. Attachment of Organic Layers to Conductive or Semiconductive Surfaces by Reduction of Diazonium Salts. *Chem. Soc. Rev.* **2005**, *34*, 429–439.
8. Kariuki, J. K.; McDermott, M. T. Nucleation and Growth of Functionalized Aryl Films on Graphite Electrodes. *Langmuir* **1999**, *15*, 6534–6540.
9. Kariuki, J. K.; McDermott, M. T. Formation of Multilayers on Glassy Carbon Electrodes *via* the Reduction of Diazonium Salts. *Langmuir* **2001**, *17*, 5947–5951.
10. Liu, Y.-C.; McCreery, R. L. Raman Spectroscopic Determination of the Structure and Orientation of Organic Monolayers Chemisorbed on Carbon Electrode Surfaces. *Anal. Chem.* **1997**, *69*, 2091–2097.
11. Combellas, C.; Kanoufi, F.; Pinson, J.; Podvorica, F. I. Time-of-Flight Secondary Ion Mass Spectroscopy Characterization of the Covalent Bonding between a Carbon Surface and Aryl Groups. *Langmuir* **2005**, *21*, 280–286.
12. Boukerma, K.; Chehimi, M. M.; Pinson, J.; Blomfield, C. X-ray Photoelectron Spectroscopy Evidence for the Covalent Bond between an Iron Surface and Aryl Groups Attached by the Electrochemical Reduction of Diazonium Salts. *Langmuir* **2003**, *19*, 6333–6335.
13. Hurley, B. L.; McCreery, R. L. Covalent Bonding of Organic Molecules to Cu and Al Alloy 2024 T3 Surfaces *via* Diazonium Ion Reduction. *J. Electrochem. Soc.* **2004**, *151*, B252–B259.
14. Bernard, M. C.; Chausse, A.; Cabet-Deliry, E.; Chehimi, M. M.; Pinson, J.; Podvorica, F.; Vautrin-Ul, C. Organic Layers Bonded to Industrial, Coinage, and Noble Metals through Electrochemical Reduction of Aryldiazonium Salts. *Chem. Mater.* **2003**, *15*, 3450–3462.
15. Laforgue, A.; Addou, T.; Belanger, D. Characterization of the Deposition of Organic Molecules at the Surface of Gold by the Electrochemical Reduction of Aryldiazonium Cations. *Langmuir* **2005**, *21*, 6855–6865.
16. Ricci, A.; Bonazzola, C.; Calvo, E. J. An FT-IRRAS Study of Nitrophenyl Mono- and Multilayers Electro-deposited on Gold by Reduction of the Diazonium Salt. *Phys. Chem. Chem. Phys.* **2006**, *8*, 4297–4299.
17. Liu, G. Z.; Bocking, T.; Gooding, J. J. Diazonium Salts: Stable Monolayers on Gold Electrodes for Sensing Applications. *J. Electoanal. Chem.* **2007**, *600*, 335–344.
18. Paulik, M. G.; Brooksby, P. A.; Abell, A. D.; Downard, A. J. Grafting Aryl Diazonium Cations to Polycrystalline Gold: Insights into Film Structure Using Gold Oxide Reduction, Redox Probe Electrochemistry, and Contact Angle Behavior. *J. Phys. Chem. C* **2007**, *111*, 7808–7815.
19. Shewchuk, D. M.; McDermott, M. T. Comparison of Diazonium Salt Derived and Thiol Derived Nitrobenzene Layers on Gold. *Langmuir* **2009**, *25*, 4556–4563.
20. Lehr, J.; Williamson, B. E.; Flavel, B. S.; Downard, A. J. Reaction of Gold Substrates with Diazonium Salts in Acidic Solution at Open-Circuit Potential. *Langmuir* **2009**, *25*, 13503–13509.
21. Brust, M.; Fink, J.; Bethell, D.; Schiffrin, D. J.; Kiely, C. Synthesis and Reactions of Functionalized Gold Nanoparticles. *J. Chem. Soc., Chem. Commun.* **1995**, 1655–1656.
22. Ni, J.; Lipert, R. J.; Dawson, G. B.; Porter, M. D. Immunoassay Readout Method Using Extrinsic Raman Labels Adsorbed on Immunogold Colloids. *Anal. Chem.* **1999**, *71*, 4903–4908.
23. Mirkhalaf, F.; Paprotny, J.; Schiffrin, D. J. Synthesis of Metal Nanoparticles Stabilized by Metal−Carbon Bonds. *J. Am. Chem. Soc.* **2006**, *128*, 7400–7401.
24. Ghosh, D.; Chen, S. W. Palladium Nanoparticles Passivated by Metal−Carbon Covalent Linkages. *J. Mater. Chem.* **2008**, *18*, 755–762.
25. Mangeney, C.; Qin, Z.; Dahoumane, S. A.; Adenier, A.; Herbst, F.; Boudou, J. P.; Pinson, J.; Chehimi, M. M. Electroless Ultrasonic Functionalization of Diamond Nanoparticles Using Aryl Diazonium Salts. *Diamond Relat. Mater.* **2008**, *17*, 1881–1887.
26. Adenier, A.; Cabet-Deliry, E.; Chausse, A.; Griveau, S.; Mercier, F.; Pinson, J.; Vautrin-Ul, C. Grafting of Nitrophenyl Groups on Carbon and Metallic Surfaces without Electrochemical Induction. *Chem. Mater.* **2005**, *17*, 491–501.

27. Malinsky, M. D.; Kelly, K. L.; Schatz, G. C.; Van Duyne, R. P. Chain Length Dependence and Sensing Capabilities of the Localized Surface Plasmon Resonance of Silver Nanoparticles Chemically Modified with Alkanethiol Self-Assembled Monolayers. *J. Am. Chem. Soc.* **2001**, *123*, 1471–1482.
28. Weisbecker, C. S.; Merritt, M. V.; Whitesides, G. M. Molecular Self-Assembly of Aliphatic Thiols on Gold Colloids. *Langmuir* **1996**, *12*, 3763–3772.
29. Porter, M. D.; Lipert, R. J.; Siperko, L. M.; Wang, G.; Narayanan, R. SERS as a Bioassay Platform: Fundamentals, Design, and Applications. *Chem. Soc. Rev.* **2008**, *37*, 1001–1011.
30. Clarkson, J.; Smith, W. E. A DFT Analysis of the Vibrational Spectra of Nitrobenzene. *J. Mol. Struct.* **2003**, *655*, 413–422.
31. Skadtchenko, B. O.; Aroca, R. Surface-Enhanced Raman Scattering of *p*-Nitrothiophenol Molecular Vibrations of Its Silver Salt and the Surface Complex Formed on Silver Islands and Colloids. *Spectrochim. Acta, Part A* **2001**, *57*, 1009–1016.
32. Fielicke, A.; von Helden, G.; Meijer, G.; Pedersen, D. B.; Simard, B.; Rayner, D. M. Gold Cluster Carbonyls: Saturated Adsorption of CO on Gold Cluster Cations, Vibrational Spectroscopy, and Implications for Their Structures. *J. Am. Chem. Soc.* **2005**, *127*, 8416–8423.
33. Baltruschat, H.; Heitbaum, J. On the Potential Dependence of the Cn Stretch Frequency on Au Electrodes Studied by Sers. *J. Electroanal. Chem.* **1983**, *157*, 319–326.
34. Beltramo, G. L.; Shubina, T. E.; Mitchell, S. J.; Koper, M. T. M. Cyanide Adsorption on Gold Electrodes: A Combined Surface Enhanced Raman Spectroscopy and Density Functional Theory Study. *J. Electroanal. Chem.* **2004**, *563*, 111–120.
35. Watling, K.; Hope, G. A.; Woods, R. SERS Investigation of Gold Dissolution in Chloride and Cyanide Media. *J. Electrochem. Soc.* **2005**, *152*, D103–D108.
36. Bozzini, B.; D'Urzo, L.; Mele, C.; Romanello, V. A SERS Investigation of Cyanide Adsorption and Reactivity during the Electrodeposition of Gold, Silver, and Copper from Aqueous Cyanocomplexes Solutions. *J. Phys. Chem. C* **2008**, *112*, 6352–6358.
37. Jiang, D. E.; Sumpter, B. G.; Dai, S. Structure and Bonding between an Aryl Group and Metal Surfaces. *J. Am. Chem. Soc.* **2006**, *128*, 6030–6031.
38. de la Llave, E.; Ricci, A.; Calvo, E. J.; Scherlis, D. A. Binding between Carbon and the Au(111) Surface and What Makes It Different from The S−Au(111) Bond. *J. Phys. Chem. C* **2008**, *112*, 17611–17617.
39. Zhao, J.; Dieringer, J. A.; Zhang, X. Y.; Schatz, G. C.; Van Duyne, R. P. Wavelength-Scanned Surface-Enhanced Resonance Raman Excitation Spectroscopy. *J. Phys. Chem. C* **2008**, *112*, 19302–19310.
40. Zhao, L. L.; Jensen, L.; Schatz, G. C. Pyridine-Ag-20 Cluster: A Model System for Studying Surface-Enhanced Raman Scattering. *J. Am. Chem. Soc.* **2006**, *128*, 2911–2919.
41. Aikens, C. M.; Schatz, G. C. TDDFT Studies of Absorption and SERS Spectra of Pyridine Interacting with Au-20. *J. Phys. Chem. A* **2006**, *110*, 13317–13324.
42. Whelan, C. M.; Barnes, C. J.; Walker, C. G. H.; Brown, N. M. D. Benzenethiol Adsorption on Au(111) Studied by Synchrotron ARUPS, HREELS and XPS. *Surf. Sci.* **1999**, *425*, 195–211.
43. Becke, A. D. Density-Functional Exchange-Energy Approximation with Correct Asymptotic-Behavior. *Phys. Rev. A* **1988**, *38*, 3098–3100.
44. Perdew, J. P. Density-Functional Approximation for the Correlation-Energy of the Inhomogeneous Electron-Gas. *Phys. Rev. B* **1986**, *33*, 8822–8824.
45. Frisch, M. J.; Trucks, G. W.; Schlegel, H. B.; Scuseria, G. E.; Robb, M. A.; Cheeseman, J. R.; Scalmani, G.; Barone, V.; Mennucci, B.; Petersson, G. A.; *et al. Gaussian 09*; Gaussian, Inc.: Wallingford, CT, 2009.
46. Neugebauer, J.; Hess, B. A. Fundamental Vibrational Frequencies of Small Polyatomic Molecules from Density-Functional Calculations and Vibrational Perturbation Theory. *J. Chem. Phys.* **2003**, *118*, 7215–7225.
47. Perdew, J. P.; Burke, K.; Ernzerhof, M. Generalized Gradient Approximation Made Simple. *Phys. Rev. Lett.* **1996**, *77*, 3865–3868.
48. Andrae, D.; Haussermann, U.; Dolg, M.; Stoll, H.; Preuss, H. Energy-Adjusted *Ab Initio* Pseudopotentials for the 2nd and 3rd Row Transition-Elements. *Theor. Chim. Acta* **1990**, *77*, 123–141.
49. Mclean, A. D.; Chandler, G. S. Contracted Gaussian-Basis Sets for Molecular Calculations 0.1. 2nd Row Atoms, $Z = 11-18$. *J. Chem. Phys.* **1980**, *72*, 5639–5648.
50. Krishnan, R.; Binkley, J. S.; Seeger, R.; Pople, J. A. Self-Consistent Molecular-Orbital Methods 0.20. Basis Set for Correlated Wave-Functions. *J. Chem. Phys.* **1980**, *72*, 650–654.